

Effects of biological treatment and particle size on properties and microstructure of microbial cemented recycled aggregate filling materials (MCRB)

Yuxin Wang, Jie Cui, Shihua Liang, Deluan Feng, Yadong Li, Yi Shan

Civil Engineering and Transportation, Guangzhou University, Guangzhou, China, 112416002wyx@e.gzhu.edu.cn

ABSTRACT: Construction and demolition waste (CDW), due to their complex composition, brittle particles, and cracked surfaces, exhibit significant differences from natural sand in terms of mineral composition, physicochemical properties, and mechanical performance. However, they offer distinct environmental benefits. To improve the processing efficiency of recycled aggregates, this study employs Microbially induced carbonate precipitation (MICP) technology as an alternative to cement as a binder. Microbial cemented recycled aggregate filling materials (MCRB) are prepared, and the effects of particle size, failure modes, and microstructure of MCRB are examined. The results show that: (1) Particle gradation plays a dominant role in MCRB, and well-graded aggregates can compensate for some of the performance deficiencies of recycled aggregates. (2) With an increasing number of MICP treatment cycles, the porosity of individual recycled aggregate particles significantly decreases, and pores within the range of 10^{-2} to 10^2 μm are substantially reduced, leading to notable improvements in the microstructure of the recycled aggregates and optimizing the pore size distribution within the samples. By optimizing the pore structure of recycled aggregates through MICP and carefully adjusting their gradation, the materials meet the requirements for backfill applications. This research provides valuable data and innovative solutions for the sustainable processing and recycling of recycled aggregates, contributing significantly to promoting a circular economy.

KEYWORDS: Microbially induced calcium carbonate precipitation (MICP), recycled aggregate, particle size, low-field nuclear magnetic resonance (LF-NMR), micro-pore structure.

1 INTRODUCTION

As a pivotal sector of the national economy, the construction and building materials industry exerts substantial influence on both the environment and ecological systems (Hwang & Zong, 2011). The global construction industry produces over 3 billion tons of construction and demolition waste (CDW) every year, which poses a serious challenge to the environment and resources, resulting in huge environmental pressure and resource consumption (Pu et al., 2023). Landfilling, characterized by its simplicity and relatively low cost, remains a widely adopted method for disposing of CDW. Improper landfilling practices can result in irreversible environmental pollution and trigger severe geotechnical hazards, such as foundation subsidence and unstable landslides, which pose serious risks to public safety (Zhan et al., 2021). Recycling CDW into recycled aggregates (RA) is a critical strategy for achieving the United Nations Sustainable Development Goals. However, RAs exhibit inherent limitations when compared to natural aggregates (NA), including higher porosity, lower density, greater water absorption, and weaker interfacial transition zones. These shortcomings restrict their application in structural components and high-performance backfill materials (Kumar et al., 2023; Wu et al., 2023). The primary causes of these defects stem from residual mortar adhering to the surfaces and microcracks of particles present within the material.

To address these limitations, researchers have explored various enhancement techniques, among which microbial-induced calcium carbonate precipitation (MICP) has emerged as promising biotechnology (Zhao et al., 2023). MICP leverages microbial metabolism to produce urease, which catalyzes the hydrolysis of urea into carbonate ions (Feng et al., 2023). These ions subsequently react with calcium ions to form calcium carbonate precipitates, using microbial cells as nucleation sites (Abo-El-Enein et al., 2012). The resulting calcium carbonate crystals fill pore spaces and microcracks, forming a continuous mineral matrix that enhances material compactness (Zhao et al., 2025). This technique offers advantages of energy conservation, environmental sustainability, low cost, and no secondary pollution (Huang et al., 2022). The implementation of MICP technology enhances soil performance through calcite precipitation, effectively improving critical properties such as

shear (Feng et al., 2024) and compressive strength (Liang et al., 2022), liquefaction and erosion resistance (Shan et al., 2025), and small-strain stiffness (Shan et al., 2022). Numerous studies have investigated MICP treatment on soils with varying particle sizes and compositions. It has been shown that the calcium carbonate crystals formed during MICP are relatively large, making the process particularly effective for coarse-grained sands. In finer sands, pore spaces are more readily filled with calcium carbonate, resulting in a higher proportion of structurally effective bonding and denser precipitation, thereby improving interparticle cohesion (Ouyang et al., 2022). For samples composed of fine particles, the permeability coefficient tends to decrease rapidly in the early stages of MICP treatment as pore structures are progressively filled with calcite precipitates (Soon et al., 2014), leading to significant improvements in strength and stiffness (Dhami et al., 2016). When coarse particles dominate the mixture, the addition of finer particles can enhance the effectiveness of MICP-induced cementation, with optimal mechanical performance observed at specific fine particle contents (Mahawish et al., 2018). These findings highlight the critical influence of particle size distribution and soil gradation on the pore structure, bonding behavior, and overall performance of MICP treated sand. However, experimental studies on MICP treated sand with varying particle characteristics remain fragmented and lack a unified framework.

2 TEST MATERIALS AND TEST METHODS

2.1 Test materials

2.1.1 Bacteria and cementing solution used in the test

The microbial strain used in this experiment is *Sporosarcina pasteurii*. This strain was activated and inoculated into a liquid medium, which was then incubated under constant temperature and shaking to allow for expanded cultivation, producing the inoculum for the experiment. The average urease activity of the strain was 1.474 mmol/L/min, which indicates the rate at which the microorganism catalyzes the hydrolysis of urea. The biomass concentration of the inoculum was quantified by measuring the absorbance at 600 nm (OD₆₀₀), with an average value of 1.628, and the pH was adjusted to 8.0. The cementation solution was prepared by

dissolving 30 g/L urea, 55 g/L anhydrous calcium chloride, and 10 g/L ammonium chloride in purified water, resulting in a final concentration of 1 mol/L. To prevent the formation of amorphous calcium carbonate, the pH of the cementation solution was adjusted to 6.0, which favors the precipitation of crystalline calcium carbonate.

2.1.2 CDW

The CDW used in this paper is the recycled aggregate mixture after crushing the concrete pavement with the original design strength of C35 of a highway, and the strength after crushing is lower than that of natural aggregate. The CDW is processed, and it is passed through a 2 mm sieve. The main components, particle size distribution curves and XRD results are shown in Figure 1, Figure 2 and Table 1.

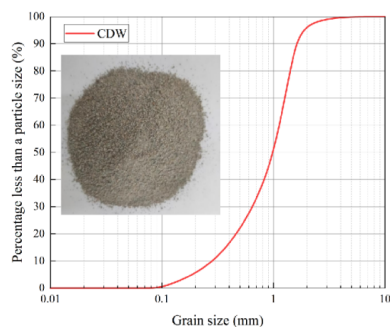


Figure 1. Grading curve of sand particle

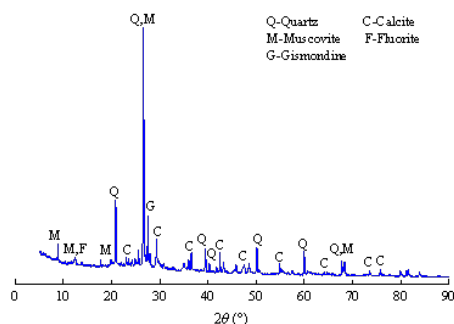


Figure 2. XRD diagram of CDW

Table 1. The main components of CDW

| Chemical compound | Content (%) |
|--------------------------------|-------------|
| SiO ₂ | 86.39 |
| MgO | 3.77 |
| Al ₂ O ₃ | 3.09 |
| CaO | 2.56 |
| P ₂ O ₅ | 1.35 |
| Fe ₂ O ₃ | 1.27 |
| K ₂ O | 1.08 |
| Other | 0.49 |

2.2 Test scheme and methods

To investigate the influence of MICP on the strength characteristics and treatment mechanism of microbial cemented recycled aggregate filling materials (MCRB), this study systematically investigated the influence of sand particle size on the treatment effect. In preliminary tests, we found that samples with particle sizes of Gradation range 0.1-0.5 mm (Fine particle size group, Group F) showed extremely uneven microbial cementation and had poor treated effect. Smaller particles had smaller pores and microcracks, slowing the flow of the bacterial and cementing solutions, causing blockages and

preventing successful treatment, leading to unsuccessful treatment. Finer particles also hinder microbial migration between pores, resulting in uneven calcium carbonate deposition (Mitchell & Santamarina, 2005; Mortensen et al., 2011; Tang et al., 2020). To minimize potential misunderstandings and enhance the research value, the variable affecting the range of 0.1-0.5 mm (Group F) was excluded.

The CDW used in the test was sieved to create sand samples with different particle size distributions, as shown in Table 2. Each sample underwent 50 mL of bacteria solution and cementation solution injections during each round, with the injection rate set to 1 mL/min. Three parallel samples were prepared for each group to minimize experimental errors. Each sample underwent three rounds of injections, with the bacteria solution injected in the first round and the nutrient solution injected every 8 hours for a total of 9 injections. The samples were fully treated and then dried in an oven at 105 °C for 24 hours. Following the Chinese geotechnical testing method standards GB/T 50123-2019 (China & Institute, 2019), unconfined compressive strength test (UCS), calcium carbonate content test, water absorption test and micro phase analysis test of MCRB were carried out.

Table 2. Test scheme

| Gr. | Test group category | Gradation range/mm | Particle size distribution | Mean d./mm |
|-----|-----------------------|--------------------|----------------------------|------------|
| U | Uniform particle size | 0.1-2.0 | Uniformly gradation | 1.12 |
| S | Small particle size | 0.5-1.0 | Single gradation | 0.75 |
| M | Medium particle size | 1.0-1.5 | Single gradation | 1.25 |
| C | Coarse particle size | 1.5-2.0 | Single gradation | 1.75 |

3 RESULTS AND ANALYSIS

3.1 Mechanical performance testing and analysis

3.1.1 UCS test

The UCS of MCRB samples with varying particle size distributions is shown in Figure 3. The UCS of the U group reached 0.37 MPa, while the highest strength was observed in the C group (0.40 MPa), and the lowest in the S group (0.17 MPa). The U and C groups exhibited relatively higher strength. All samples failed in a brittle manner, although the U group showed slightly better ductility. Differences in particle size significantly influenced the formation of pore structures. Coarse particles tended to form macropores with higher connectivity, whereas fine particles produced micropores with limited interconnectivity. In the S and M groups, the irregular morphology of CDW particles resulted in closed internal pores and non-uniform contact surfaces. As a result, fluid pathways were often blocked, causing calcium carbonate to preferentially accumulate on particle surfaces rather than in interparticle voids. This limited the development of effective bonding between particles, reducing the cementation efficiency and ultimately lowering the UCS. By contrast, the coarse particles in the C and S groups demonstrated higher packing density and roughness of surface due to their angular geometry. These features provided favorable nucleation sites for calcium carbonate, which precipitated into microcracks and coated particle surfaces. The increased surface area and interparticle spacing promoted microbial attachment and growth, leading to the formation of denser and stronger calcium carbonate bridges. When the pore size is excessively large, as observed in coarser particles, the increased permeability reduces microbial retention time. This hindered in-situ calcium carbonate precipitation and weakened the cementation effect. Thus,

although coarse particles improve mechanical interlocking and microscale strength, overly open pore structures may reduce treatment efficacy. Well-graded CDW can effectively mitigate the mechanical disadvantages associated with RA and improve the performance of MRCB.

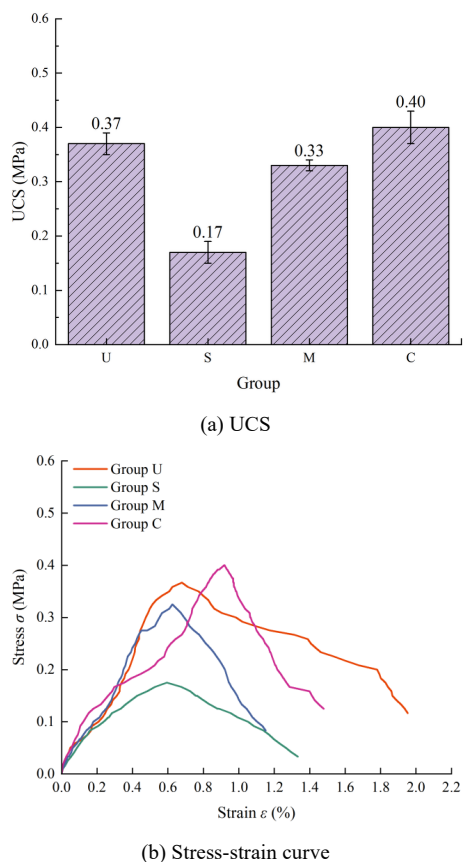


Figure 3. Comparison of UCS and stress-strain laws of MRCB in different particle size ranges

3.1.2 Calcium carbonate content test

The effects of particle size distribution on calcium carbonate content are shown in Figure 4. The calcium carbonate content of MRCB samples ranged from 15.38% to 17.23%. This relatively high deposition is attributed to the heterogeneous composition of CDW. The CDW used in this study contained 2.56% CaO, providing an intrinsic calcium source that could participate in the MICP process. During microbial-induced calcium carbonate precipitation, calcium ions react with carbonate ions generated by urease hydrolysis, leading to the formation of calcium carbonate. CDW particles typically exhibit complex pore networks and abundant microcracks, which act as primary pathways for water and nutrient transport. These microcracks provide favorable interfaces and channels for microbial colonization and metabolic activity. Microorganisms preferentially migrate into these microcracks and utilize internal calcium sources to induce localized calcium carbonate precipitation. Moreover, microbial cells strongly adhere to microcrack surfaces due to extracellular polymeric substances (EPS), which enhance microbial retention in the CDW matrix. The high surface energy and numerous adsorption sites in microcracks facilitate microbial accumulation and promote efficient mineralization. These microenvironments support the nucleation and growth of calcium carbonate crystals, leading to improved overall deposition.

The observed inverse correlation between the measured UCS and the content of precipitated calcium carbonate is a

noteworthy finding, which underscores the paramount importance of cementation distribution over sheer cementation quantity. The Group C exhibited the highest strength despite a moderate increase in CaCO_3 , because the large interparticle pores facilitated the optimal delivery of bacterial and cementation solutions. This likely resulted in the preferential precipitation of calcite at the critical interparticle contacts, effectively “welding” the grains together and reinforcing the inherently strong granular skeleton (Mahat, 2019). In contrast, the finer-grained matrices, while potentially accommodating a higher total mass of CaCO_3 due to their larger specific surface area, promote a less efficient surface coating and pore-filling mode of precipitation. This non-structural form of cementation does little to enhance particle interlocking, leading to a disproportionately lower strength gain per unit of precipitated carbonate (Joshi et al., 2026). Consequently, the treatment efficiency of MICP is not solely a function of the biomineral mass, but is predominantly controlled by the pore-scale geometry that dictates the distribution pattern of the cementing agent.

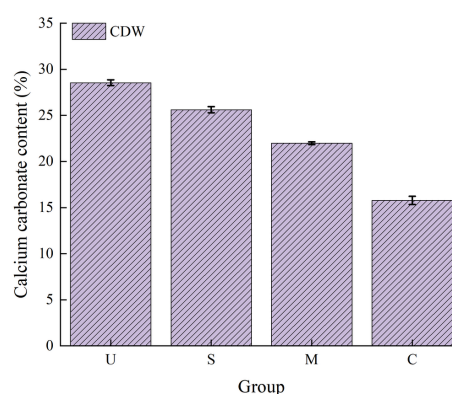


Figure 4. Comparison of calcium carbonate content of MRCB in different particle size ranges

Sand particles of different particle size ranges form pores of varying sizes, and differences in grading and compactness affect the connectivity and distribution of these pores, as shown in Figure 5. If the pore structure of the soil cannot provide sufficient space and channels, the microorganisms will not be able to effectively contact and interact with the soil particles, thereby reducing the treated effect. This is the main reason why group F cannot be treated. When particle grading is more uniform and the particle size distribution is narrower, pore connectivity improves, which enhances the uniformity of the MICP process and promotes calcium carbonate precipitation. Uniform grading and smaller particle size distributions facilitate closer particle contact, increasing the reaction surface area and allowing microorganisms to more effectively interact with the particles (Ji et al., 2024), thereby fostering calcium carbonate deposition. Additionally, better pore connectivity facilitates the even distribution and movement of moisture, ensuring smooth transport of calcium sources and carbonate ions into the particles, enabling the MICP reaction to proceed uniformly throughout the particle assembly. CDW with larger particle sizes generally has a larger surface area and more complex pore structures, offering more interfaces for reactions. This supports the reaction between microbial metabolic products and the calcium in the CDW, resulting in the formation of calcium carbonate.

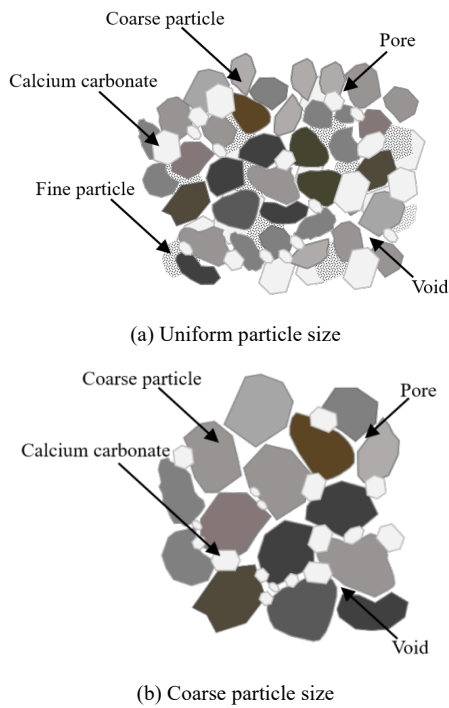


Figure 5. The schematic diagram of MICP treated in different particle size ranges

3.1.3 Water absorption test

As shown in Figure 6, the water absorption rate of MCRB samples increased by 6.85% to 32.91%. This elevated absorption is primarily attributed to the high content of hardened mortar on the surface of CDW particles, which is inherently porous. Additionally, the irregular shapes, uneven particle size distribution, and abundant microcracks in the particles further facilitated water infiltration into the particle interiors. The trend in water absorption increased from finer to medium particle size ranges, peaking in the M group, and then decreased with coarser particles. This suggests that particle size distribution plays a dominant role in influencing water absorption. Finer particles offer greater surface area for water contact and promote denser packing, resulting in more continuous pore networks and shorter pathways for water migration. These characteristics facilitate enhanced water adsorption and internal infiltration within the particle structure.

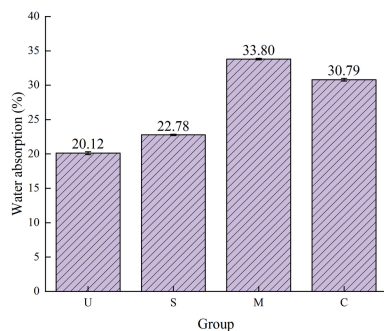


Figure 6. Comparison of water absorption of MCRB in different particle size ranges

3.2 Microscopic phase testing and analysis

3.2.1 Low-field nuclear magnetic resonance (LF-NMR) test

To assess the effectiveness of the MICP process, LF-NMR tests were performed on samples with comparable treatment levels after one to three grouting rounds. LF-NMR determines pore size distribution by detecting the water signal in saturated samples, with the calibration curve for the water volume–

nuclear magnetic signal relationship presented in Figure 7. As summarized in Table 3, both NMR-derived and gravimetric porosities significantly decreased with increasing grouting cycles, by 21.00% and 17.31%, respectively, indicating improved sample compactness. This enhancement is mainly attributed to increased pore-filling and improved pore connectivity during repeated grouting. In the MICP process, calcium carbonate precipitates are generated via microbial metabolism and reactions with calcium ions, progressively filling the pore space. As grouting rounds increase, more precipitates accumulate, further reducing porosity and enhancing inter-pore connectivity. These microstructural modifications ultimately contribute to increased mechanical strength and structural stability (Kirkland et al., 2017).

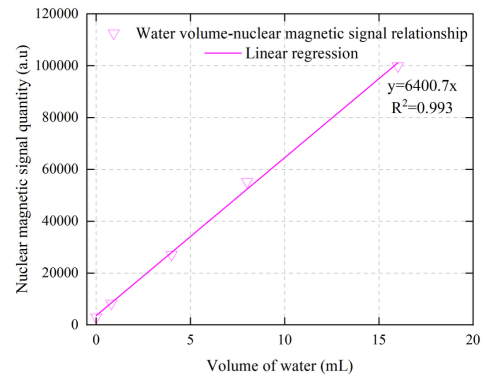


Figure 7. LR-NMR test water volume-nuclear magnetic signal relationship calibration curve

Figures 8 to 10 illustrate the progressive densification of internal structures with additional grouting. The T_2 spectra (Figure 8) exhibit a bimodal distribution centered around 0.1 ms to 1 ms and 10 ms to 100 ms. While peak positions remain unchanged, peak areas decline with more grouting, indicating a reduction in total pore volume. As illustrated in Figure 9, the pore size range evolves with grouting: from 3.57 nm to 1.23×10^4 nm (1 round) to 4.29 nm to 2.83×10^4 nm (2 rounds), and 10.83 nm to 2.17×10^5 nm (3 rounds). Micropores ($<1 \mu\text{m}$) were effectively filled after three rounds. Initially, larger surface pores were filled; subsequent rounds allowed calcium carbonate to infiltrate smaller pores, narrowing pore diameters and making the distribution more uniform. Figure 10 shows notable changes in micropore volume. For one round, most pore volume was within $0.0025 \mu\text{m}$ to $0.025 \mu\text{m}$ (63.99%). With more rounds, pores $<0.0025 \mu\text{m}$ were filled first, decreasing from 21.42% to 8.90%, followed by reductions in $1 \mu\text{m}$ to $4 \mu\text{m}$ pores (from 5.22% to 1.37%) and an increase in $0.0025 \mu\text{m}$ to $0.025 \mu\text{m}$ pores (from 42.57% to 48.09%). These findings demonstrate that calcium carbonate effectively fills internal microcracks and micropores in CDW particles, enhancing particle densification and contributing to improved overall structural integrity (Kirkland et al., 2017).

Table 3. The results of LF-NMR test data of MICP treated round grouting round changes

| Treated rounds | 1 | 2 | 3 |
|--|-------|-------|-------|
| Nuclear magnetic conversion water volume / cm^3 | 0.59 | 0.69 | 0.68 |
| Volume of sample / cm^3 | 1.36 | 1.95 | 1.98 |
| Volume of weigh water /mL | 0.61 | 0.72 | 0.73 |
| Nuclear magnetic porosity /% | 43.38 | 35.38 | 34.27 |
| Weighing porosity /% | 44.60 | 37.14 | 36.88 |

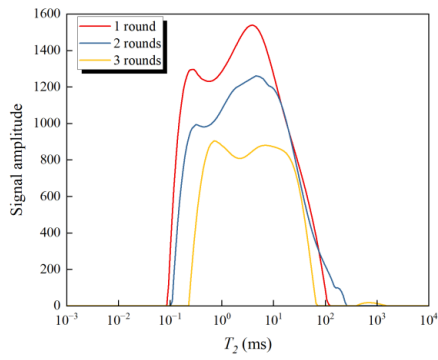


Figure 8. T_2 spectrum of grouting rounds change

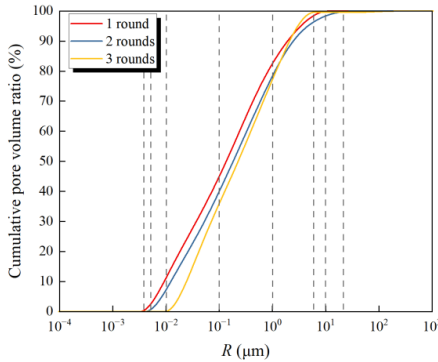


Figure 9. The cumulative distribution map of pore volume changes in grouting rounds

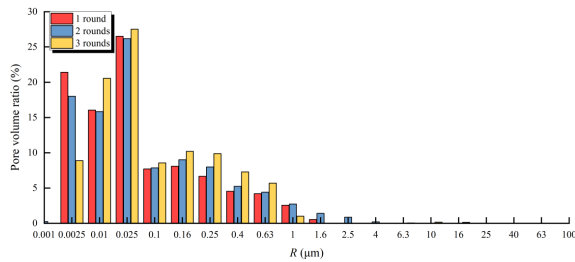


Figure 10. Histogram of pore radius distribution of grouting rounds change

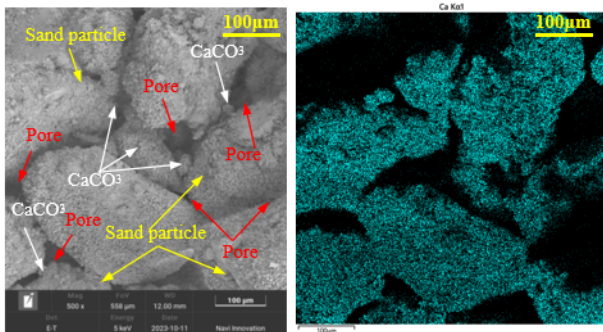
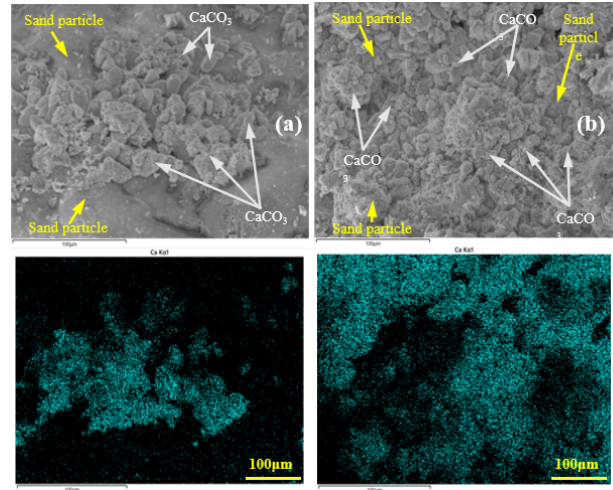


Figure 11. SEM images of MCRB

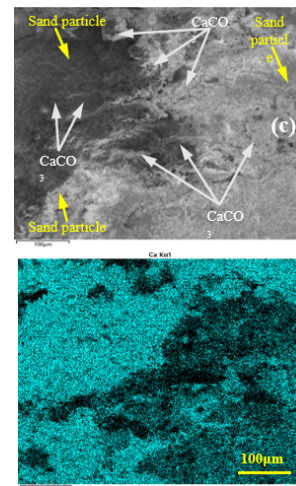
3.2.2 SEM and XRD

As shown in the SEM images (Figure 11 and Figure 12), a progressively thicker calcium carbonate coating becomes apparent with increasing grouting rounds. These precipitates gradually fill the surface micropores and inter-particle voids. A dense and uniform layer of calcium carbonate covers the CDW particle surfaces, concealing their original textures and effectively sealing microcracks and irregular voids. This coating enhances surface smoothness and fosters the development of a more continuous and well-structured mineral

matrix (Yuan et al., 2023). As grouting progresses, the initially irregular pore structures are gradually replaced by evenly distributed and structurally organized calcium carbonate deposits. The XRD patterns (Figure 13) confirm that the diffraction peak intensity of calcite significantly increases in CDW after MICP treatment. These results indicate the progressive accumulation of calcium carbonate during the treatment process advances.



(a) (b)



(c)

Figure 12. SEM images of the MICP grouting round, (a) 1 round, (b) 2 rounds, (c) 3 rounds

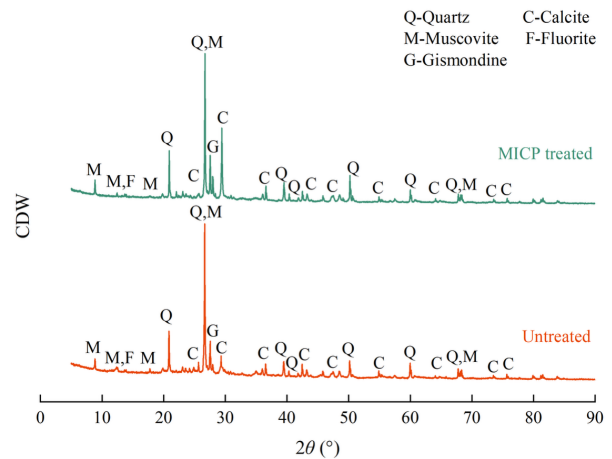


Figure 13. XRD patterns of CDW before and after MICP treated

4 CONCLUSIONS

The effects of particle size distribution and grouting rounds on microbially cemented recycled backfill (MCRB) were systematically investigated, leading to the following conclusions.

(1) MCRB samples with particle sizes ranging from 1.5 mm to 2.0 mm exhibited the highest unconfined compressive strength (UCS), reaching up to 0.40 MPa. Particle gradation exerts a dominant influence on MCRB performance, with well-graded aggregates effectively compensating for certain inherent limitations of recycled materials.

(2) MICP treatment significantly alters the pore size distribution within CDW. As the number of MICP treated rounds increases, the porosity of individual CDW particles decreases significantly. Pores in the range of 10^{-2} to $10^2 \mu\text{m}$ are substantially reduced, resulting in improved microstructure and a more favorable pore size distribution within the samples.

(3) Through the optimization of pore structure via MICP and appropriate gradation adjustment, the MCRB can meet the engineering requirements for backfill applications.

5 ACKNOWLEDGEMENTS

This work was supported by the the National Natural Science Foundation of China (Grant No. 52478332, Grant No. 52078142), and the Natural Science Foundation of Guangdong Province (Grant No. 2022A1515011047).

6 REFERENCES

Abo-El-Enain, S., Ali, A., Talkhan, F. N., & Abdel-Gawwad, H. (2012). Utilization of microbial induced calcite precipitation for sand consolidation and mortar crack remediation. *HBRC Journal*, 8(3), 185-192.

Standard for geotechnical testing method, 717 (2019). https://kns.cnki.net/kcms2/article/abstract?v=5ykJdPmCibL9GpLcXZCr0Q4iLIUemw95Oqv7GD1j_mTZaHdfd3_ltM_6Eu5BFc4K3ksuP0P8JYbv6l2kXzZmuYDs4JPXJgj365krMsPd6xCT8Y12ktSfpfgpsUgNfFYiI5WIEGGZ_mNFpMc52n-Vqxtgtuij1lbyneB5oHv0t2Xijpm5UuwAwLLbETD7YQrd&unip latform=NZKPT&language=CHS

Dhami, N. K., Reddy, M. S., & Mukherjee, A. (2016). Significant indicators for biomineralisation in sand of varying grain sizes. *Construction and Building Materials*, 104, 198-207.

Feng, C., Cui, B., Wang, J., Guo, H., Zhang, W., & Zhu, J. (2023). Changing the soaking method of microbially induced calcium carbonate precipitation technology to improve the reinforcement effect of recycled concrete aggregates. *Journal of Building Engineering*, 68, 106128.

Feng, D., Wang, Y., Chen, D., & Liang, S. (2024). Experimental study on the influence mechanism of clay particles on the microbial treatment of granite residual soil. *Construction and Building Materials*, 411, 134659.

Huang, L., Li, F., Ji, C., Wang, Y., & Yang, G. (2022). Carbon isotope fractionation and its tracer significance to carbon source during precipitation of calcium carbonate in the presence of *Bacillus cereus* LV-1. *Chemical Geology*, 609, 121029.

Hwang, B., & Zong, B. Y. (2011). Perception on benefits of construction waste management in the Singapore construction industry. *Engineering, Construction and Architectural Management*, 18(4), 394-406.

Ji, Y., Xie, L., Xiao, J., Zheng, Y., Ma, S., & Pan, T. (2024). Mechanical properties and acoustic emission characteristics of microbial cemented backfill with various particle size distributions of recycled aggregates. *Construction and Building Materials*, 417, 135269.

Joshi, P., Khosravi, M., Phillips, A., Cunningham, A., Rahn, J., Olds, S., Carter, M., & Gupta, M. (2026). Influence of Particle Size and Curing Temperature on the Strength of Sand Treated with Enzyme-Induced Carbonate Precipitation. *Journal of geotechnical and geoenvironmental engineering*, 152(2), 04025187.

Kirkland, C. M., Zanetti, S., Grunewald, E., Walsh, D. O., Codd, S. L., & Phillips, A. J. (2017). Detecting microbially induced calcite precipitation in a model well-bore using downhole low-field NMR. *Environmental Science & Technology*, 51(3), 1537-1543.

Kumar, A., Singh, G. J., Kumar, S. B., & Kumar, R. (2023). Performance-based quality optimization approach for mechanically treated recycled concrete aggregates. *Journal of Materials in Civil Engineering*, 35(9), 04023315.

Liang, S.-H., Zeng, W.-H., Feng, D.-L., Lin, J.-P., & Gong, X. (2022). Influence of polypropylene fiber on properties of biocemented calcareous sand. *Soil Mechanics and Foundation Engineering*, 59(2), 193-201.

Mahat, S. (2019). Exploring a Discrete Element Approach for Chemically Mediated Deformation at Granular Contact in Calcite Minerals (Publication Number 9781687976178) [Dissertation/Thesis, <Go to ISI>://PQDT:68746596]

Mahawish, A., Bouazza, A., & Gates, W. P. (2018). Effect of particle size distribution on the bio-cementation of coarse aggregates. *Acta Geotechnica*, 13(4), 1019-1025.

Mitchell, J. K., & Santamarina, J. C. (2005). Biological considerations in geotechnical engineering. *Journal of geotechnical and geoenvironmental engineering*, 131(10), 1222-1233.

Mortensen, B., Haber, M., DeJong, J., Caslake, L., & Nelson, D. (2011). Effects of environmental factors on microbial induced calcium carbonate precipitation. *Journal of applied microbiology*, 111(2), 338-349.

Ouyang, J., Liu, K., Sun, D., Xu, W., Wang, A., & Ma, R. (2022). A focus on Ca^{2+} supply in microbial induced carbonate precipitation and its effect on recycled aggregate. *Journal of Building Engineering*, 51, 104334.

Pu, Y., Li, L., Shi, X., Wang, Q., & Abomohra, A. (2023). A comparative life cycle assessment on recycled concrete aggregates modified by accelerated carbonation treatment and traditional methods. *Waste Management*, 172, 235-244. <https://doi.org/10.1016/j.wasman.2023.10.040>

Shan, Y., Liang, J., Tong, H., Yuan, J., & Zhao, J. (2022). Effect of different fibers on small-strain dynamic properties of microbially induced calcite precipitation-fiber combined reinforced calcareous sand. *Construction and Building Materials*, 322, 126343.

Shan, Y., Liufu, Z., Yuan, J., Li, Y., Tong, H., & Cui, J. (2025). Liquefaction resistance of MICP-treated calcareous sand with different particle size and gradation. *Biogeotechnics*, 100181.

Soon, N. W., Lee, L. M., Khun, T. C., & Ling, H. S. (2014). Factors affecting improvement in engineering properties of residual soil through microbial-induced calcite precipitation. *Journal of geotechnical and geoenvironmental engineering*, 140(5), 04014006.

Tang, C.-S., Yin, L.-y., Jiang, N.-j., Zhu, C., Zeng, H., Li, H., & Shi, B. (2020). Factors affecting the performance of microbial-induced carbonate precipitation (MICP) treated soil: a review. *Environmental Earth Sciences*, 79(5), 94.

Wu, H., Hu, R., Yang, D., & Ma, Z. (2023). Micro-macro characterizations of mortar containing construction waste fines as replacement of cement and sand: A comparative study. *Construction and Building Materials*, 383, 131328.

Yuan, J., Li, Y., Shan, Y., Tong, H., & Zhao, J. (2023). Effect of Magnesium Ions on the Mechanical Properties of Soil Reinforced by Microbially Induced Carbonate Precipitation. *Journal of Materials in Civil Engineering*, 35(11), Article 04023413. <https://doi.org/10.1061/jmce7.Mteng-15080>

Zhan, L., Guo, X., Sun, Q., Chen, Y., & Chen, Z. (2021). The 2015 Shenzhen catastrophic landslide in a construction waste dump: analyses of undrained strength and slope stability. *Acta Geotechnica*, 16(4), 1247-1263.

Zhao, J., Shan, Y., Tong, H., Yuan, J., & Liu, J. (2023). Study on calcareous sand treated by MICP in different NaCl concentrations. *European Journal of Environmental and Civil Engineering*, 27(10), 3137-3156. <https://doi.org/10.1080/19648189.2022.2130439>

Zhao, J., Tong, H., Yuan, J., Liang, S., Cui, J., & Shan, Y. (2025). Drained behavior of microbially induced calcium carbonate precipitated calcareous sand under true triaxial conditions. *Construction and Building Materials*, 490, 142546.